ISSN 0965-5425, Computational Mathematics and Mathematical Physics, 2007, Vol. 47, No. 11, pp. 1833–1855. © Pleiades Publishing, Ltd., 2007.
Original Russian Text © A.V. Mazhukin, V.I. Mazhukin, 2007, published in Zhurnal Vychislitel'noi Matematiki i Matematicheskoi Fiziki, 2007, Vol. 47, No. 11, pp. 1913–1936.

Dynamic Adaptation for Parabolic Equations

A. V. Mazhukin and V. I. Mazhukin

Institute of Mathematical Modeling,
Miusskaya pl. 4, Moscow, 125047 Russia
e-mail: immras@orc.ru

Received November 13, 2006

Abstract—A dynamic adaptation method is presented that is based on the idea of using an arbitrary time-dependent system of coordinates that moves at a velocity determined by the unknown solution. Using some model problems as examples, the generation of grids that adapt to the solution is considered for parabolic equations. Among these problems are the nonlinear heat transfer problem concerning the formation of stationary and moving temperature fronts and the convection–diffusion problems described by the nonlinear Burgers and Buckley–Leverette equations. A detailed analysis of differential approximations and numerical results shows that the idea of using an arbitrary time-dependent system of coordinates for adapted grid generation in combination with the principle of quasi-stationarity makes the dynamic adaptation method universal, effective, and algorithmically simple. The universality is achieved due to the use of an arbitrary time-dependent system of coordinates that moves at a velocity determined by the unknown solution. This universal approach makes it possible to generate adapted grids for time-dependent problems of mathematical physics with various mathematical features. Among these features are large gradients, propagation of weak and strong discontinuities in nonlinear transport and heat transfer problems, and moving contact and free boundaries in fluid dynamics. The efficiency is determined by automatically fitting the velocity of the moving nodes to the dynamics of the solution. The close relationship between the adaptation mechanism and the structure of the parabolic equations allows one to automatically control the nodes' motion so that their trajectories do not intersect. This mechanism can be applied to all parabolic equations in contrast to the hyperbolic equations, which do not include repulsive components. The simplicity of the algorithm is achieved due to the general approach to the adaptive grid generation, which is independent of the form and type of the differential equations.

DOI: 10.1134/S0965542507110097

Keywords: dynamic adaptation, principle of quasi-stationarity, grids adapted to the solution, parabolic equation, differential approximation, finite difference scheme, nonlinear heat transfer, nonlinear convection–diffusion equation

INTRODUCTION

The accuracy of a numerical solution to a partial differential equation depends on how well the distribution of the grid points corresponds to the features of the unknown solution. Optimal grids can be generated using various adaptation methods, which have been under intensive development during the last several decades (see [1–5]). The application of one or another adaptation method depends on several factors of which the main are the type of the equation or the system of equations, their dimensionality, the degree of nonlinearity, the presence of moving boundaries, and others.

The methods of adapted grid generation for elliptic equations are most developed (see [6–9]). In these methods, the grid is generated before starting the integration process. The problem of optimal distribution of the grid points is especially pressing in nonlinear time-dependent problems of mathematical physics whose solutions contain strongly nonuniformly scaled spatial variables. Such features of the solution as large gradients, transient layers, or discontinuity fronts can appear near one of the boundaries or in the interior of the domain and then expand to the entire computational domain. In such situations, it is impossible to generate a grid with the optimal distribution of nodes in advance. For that reason, grids that adapt to the unknown solution have received widespread use. Judging from the number of publications, two main approaches to adapted grid generation are currently distinguished: adaptive mesh refinement methods (AMR) and dynamically adapted grids.

The adaptive mesh refinement methods [10–12], which have lately received widespread use, are used to improve the accuracy of numerical solutions by splitting the grid cells in the regions where the solution undergoes sharp changes. This procedure may be applied repeatedly, which results in refined cells of higher orders (from third to sixth).

In the dynamic adaptation methods [15–26], which are algorithmically simpler and can deal with a constant [19, 20, 26] or variable [16, 17] number of grid points, the controlled distribution of the grid points is achieved by using information about the dynamics of the unknown solution. This allows one to concentrate more grid points in the regions where the solution undergoes sharp changes (see [19]). A close relationship between the dynamics of the solution and the location of the grid points leads to the relocation of these points at each time layer. This places more stringent requirements for matching the relocation of grid points to the dynamics of the numerical solution and for the degree of automation of the grid generation. Therefore, the algorithms that do not use fitting parameters (see [35]) have an advantage.

This paper is devoted to the definition of the general mechanism for the generation of grids that can dynamically adapt to the solutions to parabolic convection-diffusion equations (the Buckley–Leverette and Burgers equations) and the nonlinear (quasilinear) heat conduction equation. In these problems, the distribution of the grid points depends both on the moving boundaries and on the specific features of the solution in the interior of the domain.

Strongly nonlinear heat conduction leads to the occurrence of steep fixed and propagating temperature fronts.

Convection–diffusion problems appear in many mathematical models that provide the basis for fluid mechanics. These models describe the two main mechanisms of mass and energy transfer—diffusion and convection. Depending on the external conditions, each of these mechanisms can be dominating. To assess the degree of dominance of one or the other process, dimensionless parameters (the so-called Peclet (Pe) or Reynolds (Re) numbers) are used. When $\mathrm{Pe} \ll 1$ ($\mathrm{Re} \ll 1$), the diffusive process is dominating; when $\mathrm{Pe} \gg 1$ ($\mathrm{Re} \gg 1$), the convective process is dominating. When the convective transfer is strongly dominating, the class of singularly perturbed nonlinear mathematical models with a small parameter Pe^{-1} or Re^{-1} multiplying the higher order derivative is obtained. In the time-dependent singularly perturbed models, domains of a sharp change of the solution can appear that propagate in the form of various fronts and transient layers.

From the computational point of view, the singularly perturbed problems are difficult. In particular, the finite difference schemes used to approximate the convection–diffusion equations usually have a large variation, which is suppressed using special techniques.

1. STATEMENT OF THE PROBLEM

The main subject of this study is the class of time-dependent boundary value problems of mathematical physics of the form

$$\frac{\partial u}{\partial t} + \frac{\partial P(u)}{\partial x} = F^{(n)}(u), \quad x_0 < x < x_r, \quad t > 0, \tag{1.1}$$

$$t = 0\colon u(x, 0) = u^0(x), \tag{1.2}$$

$$\begin{aligned} x = x_0\colon & g_0\left(t, x_0, u(x), \frac{\partial u(x)}{\partial x}, \ldots\right) = 0, \\ x = x_r\colon & g_r\left(t, x_r, u(x), \frac{\partial u(x)}{\partial x}, \ldots\right) = 0, \end{aligned} \tag{1.3}$$

where $P(u) \geq 0$ is an intricate linear or nonlinear function, and $F^{(n)}(u) \geq 0$ is a linear or nonlinear operator of an order not higher than two ($n = 0, 1, 2$). It is assumed that the solution $u(x, t)$ and the function $u^0(x)$ are sufficiently smooth.

Depending on the form of $P(u)$ and $F^{(n)}(u)$, Eq. (1.1) can describe various physical processes and, correspondingly, be a linear or nonlinear hyperbolic or parabolic equation. For example, if

$$F^{(n)}(u) = 0, \quad P(u) = vu,$$

where $v = \mathrm{const}$, Eq. (1.1) is the simplest transport hyperbolic equation. If

$$F^{(n)}(u) = 0, \quad P(u) = u^2/2,$$

then Eq. (1.1) is the incomplete Burgers equation; it is the simplest nonlinear transport hyperbolic equation. If

$$F^{(2)}(u) = \frac{\partial}{\partial x} k(u) \frac{\partial u}{\partial x}, \quad P(u) = 0, \tag{1.4}$$

then Eq. (1.1), depending on the physical meaning of the function $k(u)$, is a quasilinear diffusion or heat conduction equation that is classified as a parabolic transport equation. If

$$F^{(2)}(u) = \mu\frac{\partial^2 u}{\partial x^2}, \quad P(u) = u^2/2, \tag{1.5}$$

where $\mu = \text{const}$, then Eq. (1.1) is the complete nonlinear Burgers equation of the parabolic type. If

$$F^{(2)}(u) = D\frac{\partial^2 u}{\partial x^2}, \quad P(u) = \frac{u^2}{u^2 + \alpha(1-u)^2}, \tag{1.6}$$

where $D, \alpha = \text{const}$, then Eq. (1.1) is the nonlinear Buckley–Leverette equation of the parabolic type.

In this paper, we use the set of differential operators (1.4)–(1.6), which make Eq. (1.1) parabolic.

2. ARBITRARY TIME-DEPENDENT SYSTEM OF COORDINATES

The dynamic adaptation method is based on the procedure of passing to an arbitrary time-dependent system of coordinates. Such a system makes it possible to formulate the problem of generation and adaptation of computational grids at the differential level. More precisely, a part of the differential equations in the resulting mathematical model describes physical processes and the other part describes the behavior of the grid points [15]. The change to the arbitrary time-dependent system of coordinates is performed by an automatic transformation of coordinates using the unknown solution.

2.1. Change of Variables

Following studies [17–20], we replace the physical space $\Omega_{x,t}$ with the Euler coordinates (x, t) by a computational space with an arbitrary time-dependent system of coordinates $\Omega_{q,\tau}$ in the variables (q, τ). This replacement can be performed using the change of variables of the general form $x = f(q, \tau)$, $t = \tau$ that has a one-valued nonsingular inverse $q = \varphi(x, t)$, $\tau = t$.

The partial derivatives of the dependent variables when we change the coordinates are related by

$$\frac{\partial}{\partial t} = \frac{\partial}{\partial \tau} + \frac{Q}{\psi}\frac{\partial}{\partial q}, \quad \frac{\partial}{\partial x} = \frac{1}{\psi}\frac{\partial}{\partial q}, \quad \frac{\partial^2}{\partial x^2} = \frac{1}{\psi}\frac{\partial}{\partial q}\frac{1}{\psi}\frac{\partial}{\partial q}, \tag{2.1}$$

where $\psi = \partial x/\partial q$ is the Jacobian of the inverse transformation.

Using the change of variables of the general form and relations (2.1), we represent the differential model (1.1)–(1.3) in the variables (q, τ) in the form

$$\frac{\partial u}{\partial \tau} + \frac{Q}{\psi}\frac{\partial u}{\partial q} + \frac{1}{\psi}\frac{\partial P(u)}{\partial q} = \frac{1}{\psi}F^{(n)}(u), \tag{2.2}$$

$$\frac{\partial x}{\partial \tau} = -Q, \tag{2.3}$$

$$q_0 < q < q_r, \quad \tau > 0,$$

where (2.3) is the equation of the inverse transformation involving the transformation function Q. The function Q, which is unknown a priori and must be found, describes the velocity of the time-dependent system of coordinates. The equation of the inverse transformation written in the form

$$\frac{\partial \psi}{\partial \tau} = -\frac{\partial Q}{\partial q}$$

is more convenient. It can be obtained by differentiating Eq. (2.3) with respect to q.

Simple manipulations reduce system (2.2), (2.3) to the conservative form

$$\frac{\partial(\psi u)}{\partial \tau} + \frac{\partial(uQ)}{\partial q} + \frac{\partial P(u)}{\partial q} = F^{(n)}(u), \tag{2.4}$$

$$\frac{\partial \psi}{\partial \tau} = -\frac{\partial Q}{\partial q}. \tag{2.5}$$

Thus, as a result of passing to the arbitrary time-dependent system of coordinates, the original differential model is transformed to the extended differential system that includes additional equation (2.3) or (2.5). Its type, properties, and the form of the boundary conditions depend on Q. At this stage of the reasoning, the function Q is unknown. As soon as it is determined, Eq. (2.5) is used to generate the grid adapted to the solution. Its difference analog describes the dynamics of the grid points, and Q controls the relocation of the grid points in coordination with the dynamics of the unknown solution. The coordination is achieved by introducing the dependence of Q on the unknown solution. However, since this solution is not known a priori, the problem of determining the optimal transformation function Q that guarantees a complete coordination of the adaptation mechanism with the solution arises. If the coordination is incomplete, some fitting coefficients are included in the control function that help to reduce the degree of incoordination. However, the use of fitting coefficients in the adaptation method indicates that it is imperfect.

2.2. The Principle of Quasi-Stationarity

The function Q determines a concrete change of coordinates and the method of controlling the relocation of the grid points. It has already been mentioned that finding the optimal function Q that ensures the relocation of the grid points fitted to the solution is a very important point in the dynamic adaptation method.

The perfect fitting implies several requirements of which the most important are the following ones:

—the distribution of the grid points depending on the specific features of the unknown solution;

—the availability of a reliable automatic control of the grid points relocation so as to prevent the intersection of their trajectories in the course of adaptation;

—the complete automation of the adaptation process, which assumes the absence of fitting parameters that change from variant to variant;

—the possibility to change the number of grid points in the course of the computations, which assumes that new nodes may be generated if needed and the redundant nodes may be eliminated.

Practical applications of dynamic adaptation (see [26–28]) show that, in order to satisfy the above requirements and ensure perfect fitting, the structure of Q must be closely related to the structure of the original equation (see [19]) or system of equations (see [27, 28]) that describe the physical process. Such a relation can be obtained using the principle of quasi-stationarity (see [19]). The idea of this principle is as follows.

When changing the coordinates, it is implicitly assumed that the time-dependent system of coordinates is chosen such that the time derivatives of the solution in the new coordinates are much smaller than in the original coordinates. A logical completion of this assumption is the requirement that the time derivatives vanish or, at least, are very small. The smallness of the time derivatives is equivalent to the requirement of the quasi-stationarity of the processes in the new system of coordinates. This point is very important because it is well known that the time derivatives play an important role in the dissipative and variation properties of finite difference schemes.

In the case of a parabolic equation, the operator $F^{(n)}$ in (1.1) is the second-order differential operator $F^{(2)} = \dfrac{\partial^2 u}{\partial x^2}$, and the equation itself has the form

$$\frac{\partial u}{\partial \tau} + \frac{Q}{\psi}\frac{\partial P(u)}{\partial q} = \frac{1}{\psi}\frac{\partial}{\partial q}\frac{1}{\psi}\frac{\partial u}{\partial q}$$

in the variables (q, τ).

Assume that we have found a system of coordinates in which $\partial u/\partial \tau = 0$. Then, the equation takes the form

$$\frac{Q}{\psi}\frac{\partial u}{\partial q} + \frac{1}{\psi}\frac{\partial P(u)}{\partial q} = \frac{1}{\psi}\frac{\partial}{\partial q}\frac{1}{\psi}\frac{\partial u}{\partial q}$$

in terms of these coordinates. Hence, we find the function Q in the form

$$Q = -\left(\frac{\partial P(u)}{\partial u} - \frac{\partial}{\partial q}\left(\frac{1}{\psi}\right) - \frac{1}{\psi}\frac{\partial^2 u/\partial q^2}{(\partial u/\partial q + \mathrm{Re})}\right), \tag{2.6}$$

where $\mathrm{Re} \ll 1$ is a regularization constant that places a lower bound on the value of the derivative $\partial u/\partial q$ when it is small.

Let us analyze (2.6). After differentiation, the first term is either the solution u or its derivative $\partial u/\partial q$ or their combination. Upon a difference approximation, this term exhibits a strong contractive action on the grid points. The third term exhibits a similar action. However, as this term is a ratio of the derivatives, its effect is much weaker compared to the effect of the first term; for that reason, it is not always taken into account. The second term exerts a repulsive action on the grid points; it provides a mechanism for an automatic control of the grid points relocation so as to prevent the intersection of their trajectories. When the distance between two adjacent grid points $(i, i + 1)$ tends to zero, the function $\psi_{i+1/2}$ for the corresponding grid cell also tends to zero. The term $\dfrac{\partial}{\partial q}\left(\dfrac{1}{\psi}\right)$ grows sharply (as $1/\psi^2$), and the repulsive effect of the function Q increases, thus, preventing the Jacobian of the transformation (the function ψ) from vanishing and the grid cells from collapsing.

Note that this mechanism of automatic control is characteristic of all parabolic equations. In the hyperbolic equations, which admit discontinuous solutions, the structure of the equations is different, and the transformation function Q obtained using the principle of quasi-stationarity and corresponding to the perfect fitting conditions does not provide a mechanism for preventing the collapse of the grid cells. For this reason, the term for exerting a repulsive action (such as $\dfrac{\partial}{\partial q}\left(\dfrac{1}{\psi}\right)$) is sometimes introduced artificially in the case of hyperbolic equations (see [20, 26]).

2.3. Initial and Boundary Conditions

As a result of passing to an arbitrary time-dependent system of coordinates, the coordinates u_i^j of the grid points become unknown in addition to the grid functions x_i^j. To find them, the extended mathematical model (2.4)–(2.6) includes partial differential equation (2.5).

Transformation of original equation (2.1) into the extended differential system (2.4)–(2.6) requires the corresponding extension of the boundary and initial conditions; that is, the quantities $\psi(0, q)$, $Q(\tau, q_0)$, and $Q(\tau, q_r)$ should be additionally specified.

The initial conditions at $\tau = \tau_0 = 0$ are determined using the following considerations. The function $\psi = \partial x/\partial q$, which is the Jacobian of the transformation, is the factor by which the geometric size of the original domain or of an individual grid size h change compared to the original values at $t = 0$. Assuming that passing to the computational domain is not associated with the deformation of the original domain, we conclude that the following conditions must be satisfied at the initial moment:

$$u(\tau_0, q) = u_0, \quad \psi(\tau_0, q) = 1 \quad \text{for} \quad \tau = \tau_0. \tag{2.7}$$

The boundary conditions for Eq. (2.4) take the form

$$\begin{aligned} g_0\left[\tau, q, u(q), \frac{1}{\psi}\frac{\partial u}{\partial q}\right] &= 0 \quad \text{for} \quad q = q_0, \\ g_r\left[\tau, q, u(q), \frac{1}{\psi}\frac{\partial u}{\partial q}\right] &= 0 \quad \text{for} \quad q = q_r. \end{aligned} \tag{2.8}$$

When formulating the boundary conditions for the equation of the inverse transformation (2.5), the conditions that are common for all types of Q must be taken into account. These conditions are as follows. All the fixed boundaries are associated with the condition $Q(\tau, q) = 0$. Any other condition ($Q(\tau, q) \neq 0$) corresponds to a moving boundary of the domain.

Using a numerical solution of some model problems describing processes of nonlinear heat conduction and convection–diffusion as examples, we show that the principle of quasi-stationarity makes it possible to determine the transformation functions Q that ensure the complete agreement of the adaptation mechanism with the unknown solution to parabolic equations.

3. NONLINEAR HEAT CONDUCTION

In heat conduction theory (see [29]), various modes of heat propagation are known depending on the thermal conditions on the boundary or on the type of nonlinear dependence of the thermal conductivity $k(u)$.

For example, it was established in [30] that the power dependence $k(u) = k_0 u^\alpha$ with $\alpha > 1$ stimulates the formation of steep temperature gradients; in the case when the thermal conductivity vanishes ($k(u) = 0$), fixed or moving temperature fronts appear (see [31, 32]) that propagate in the medium at a finite speed (see [33]) in the form of temperature waves.

Using relations (1.4) and substituting them in Eq. (1.1), we obtain the quasilinear heat conduction equation

$$\frac{\partial u}{\partial t} = -\frac{\partial W}{\partial x}, \quad W = -k(u)\frac{\partial u}{\partial x}, \qquad x_0 < x < x_r, \quad t > 0, \tag{3.1}$$

where $-k(u) = k_0 u^\alpha$, k_0 is a constant, further $k_0 = 1$, and $\alpha > 1$.

Using the change of variables of the general form and applying relation (2.1), we rewrite Eq. (3.1) in terms of the variables (q, τ) as

$$\frac{\partial u}{\partial \tau} + \frac{Q}{\psi}\frac{\partial u}{\partial q} = -\frac{1}{\psi}\frac{\partial W}{\partial q}, \quad W = -\frac{k(u)}{\psi}\frac{\partial u}{\partial q}, \tag{3.2}$$

$$\frac{\partial \psi}{\partial \tau} = -\frac{\partial Q}{\partial q}, \quad \frac{\partial x}{\partial q} = \psi, \qquad q_0 < q < q_r, \quad \tau > 0. \tag{3.3}$$

Upon a discretization of the differential model, the inverse transformation equation (3.3) is used for grid generation.

Applying the principle of quasi-stationarity $\partial u/\partial \tau = 0$ to Eq. (3.2), we determine the transformation function Q in the form

$$\begin{aligned} Q &= -\left(\frac{\partial W}{\partial q}\right)\left(\frac{\partial u}{\partial q}\right)^{-1} = \frac{\partial}{\partial q}\left(\frac{k(u)}{\psi}\right) + \frac{k(u)}{\psi}\left(\frac{\partial^2 u}{\partial q^2}\right)\left(\frac{\partial u}{\partial q} + \mathrm{Re}\right)^{-1} \\ &= \frac{\alpha u^{\alpha-1}}{\psi}\frac{\partial u}{\partial q} + u^\alpha \frac{\partial}{\partial q}\left(\frac{1}{\psi}\right) + \frac{u^\alpha}{\psi}\left(\frac{\partial^2 u}{\partial q^2}\right)\left(\frac{\partial u}{\partial q} + \mathrm{Re}\right)^{-1}. \end{aligned} \tag{3.4}$$

It has already been mentioned that the first and the third terms in (3.4) exert a contraction action on the grid points in the regions where the gradients are high. The second term restricts the mutual approach of two adjacent grid points. Its repulsive action grows sharply when ψ is small, thus, preventing ψ from vanishing and the trajectories of the grid points from intersecting.

The expression for Q and its usefulness are subject to an analytical and numerical analysis. We show that the function defined by this expression is optimal in terms of the quality of the solution under a minimum number of grid points.

3.1. Differential Approximation of Finite Difference Schemes

The use of finite difference schemes reduces the numerical solution to the original partial differential equation to the numerical solution to a modified equation called the differential approximation of the difference scheme (see [34, 35]). The right-hand side of this approximation is the error of the approximation; it is equal to the difference between the original partial differential equation and its finite dimensional analog. An analysis of the right-hand sides of differential approximations determines the prevailing contribution of the higher order derivatives and the related properties of difference schemes (such as dissipation and variation) to the approximation error. It is well known that, if the main term in the expression of the approximation error contains derivatives of an odd order, then the prevailing properties of the difference scheme are dissipative; otherwise, the prevailing properties are of the variation nature.

In time-dependent systems of coordinates, the right-hand sides of differential approximations depend on the velocity, which sometimes makes it possible to control the quality of difference schemes by a proper choice of the coordinate transformation.

In the discrete space $\Omega_{q,\tau}$, define the computational grid

$$\omega_h^{\Delta\tau} = ((q_i, \tau^j);\ q_{i+1} = q_i + h,\ \tau^{j+1} = \tau^j + \Delta\tau^j,\ i = 0, 1, \ldots, N-1,\ j = 0, 1, \ldots, J)$$

and consider the family of three finite difference schemes approximating Eq. (3.2) taking into account the condition $\partial u/\partial\tau = 0$: the scheme based on the central difference quotients

$$Q_i\frac{u_{i+1}-u_{i-1}}{2h}-\frac{1}{h}\left(\left(\frac{k}{\Psi}\right)_{i+1/2}\frac{u_{i+1}-u_i}{h}-\left(\frac{k}{\Psi}\right)_{i-1/2}\frac{u_i-u_{i-1}}{h}\right)=0; \tag{3.5}$$

the scheme based on the forward difference quotients

$$Q_i\frac{u_{i+1}-u_i}{h}-\frac{1}{h}\left(\left(\frac{k}{\Psi}\right)_{i+1/2}\frac{u_{i+1}-u_i}{h}-\left(\frac{k}{\Psi}\right)_{i-1/2}\frac{u_i-u_{i-1}}{h}\right)=0; \tag{3.6}$$

and the scheme based on the backward difference quotients

$$Q_i\frac{u_i-u_{i-1}}{h}-\frac{1}{h}\left(\left(\frac{k}{\Psi}\right)_{i+1/2}\frac{u_{i+1}-u_i}{h}-\left(\frac{k}{\Psi}\right)_{i-1/2}\frac{u_i-u_{i-1}}{h}\right)=0. \tag{3.7}$$

Each of these schemes consists of a finite number of algebraic equations for grid functions that approximate differential equation (3.2) up to a certain degree of accuracy. In some cases, the differences between the differential model and its difference analog can be significant; generally, these differences require a special analysis.

Let us write out the differential approximations for schemes (3.5)–(3.7). To obtain them, we use the standard procedure of expanding grid functions in the Taylor series about the point (i). Simple but tedious calculations yield the following expressions for the differential approximations for schemes (3.5)–(3.7), which differ from each other only by the coefficients on the right-hand side:

$$Q\frac{\partial u}{\partial q}-\frac{\partial}{\partial q}\left(\frac{k(u)}{\psi}\frac{\partial u}{\partial q}\right)=\delta_n\frac{\partial u}{\partial q}+\alpha_n\frac{\partial^2 u}{\partial q^2}+\beta_n\frac{\partial^3 u}{\partial q^3}+\gamma_n\frac{\partial^4 u}{\partial q^4},\quad n=1,2,3. \tag{3.8}$$

For the scheme based on the central difference quotients ($n = 1$), we have

$$\delta_1=\frac{h^2}{24}\frac{\partial^3}{\partial q^3}\left(\frac{k(u)}{\psi}\right),\quad \alpha_1=\frac{h^2}{8}\frac{\partial^2}{\partial q^2}\left(\frac{k(u)}{\psi}\right),\quad \beta_1=-\frac{h^2}{6}\left(Q-\frac{\partial}{\partial q}\left(\frac{k(u)}{\psi}\right)\right),\quad \gamma_1=\frac{h^2}{12}\frac{k(u)}{\psi}.$$

For the schemes based on the forward ($n = 2$, see (3.6)) and backward ($n = 3$, see (3.7)) difference quotients, the differential approximations differ from each other only by the sign on the right-hand side:

$$\delta_{2,3}=\delta_1,\quad \alpha_{2,3}=\alpha_0+\alpha_1,\quad \alpha_0=\mp\frac{h}{2}Q,\quad \beta_{2,3}=\beta_1,\quad \gamma_{2,3}=\gamma_1.$$

In these expressions, the index 2 corresponds to the equation for scheme (3.6), and the index 3 corresponds to the differential approximation of scheme (3.7). The upper sign in the coefficients $\delta_{2,3}$ and $\alpha_{2,3}$ corresponds to the first index and the lower sign corresponds to the second index.

Let us analyze the coefficients multiplying the derivatives on the right-hand side of the differential approximations. The most important role is played by the coefficient β multiplying the third-order derivative; it determines the variation of the corresponding difference scheme. For the entire family of difference schemes under examination, β has the same form. It can be easily made equal to zero by choosing Q in the form

$$Q=\frac{\partial}{\partial q}\left(\frac{k(u)}{\psi}\right)=\frac{\alpha u^{\alpha-1}}{\psi}\frac{\partial u}{\partial q}+u^{\alpha}\frac{\partial}{\partial q}\left(\frac{1}{\psi}\right). \tag{3.9}$$

Expression (3.9) is shorter by one term than expression (3.4), and it allows us to completely eliminate the internal variation of the difference schemes. A specific feature of the other coefficients is that they depend on the nonlinear thermal conductivity $k(u)$. Large gradients of the solution appear in a neighborhood of the points where $k(u) \longrightarrow 0$. However, due to the dependence of the coefficients δ, α, and γ on $k(u)$, their values also tend to zero, thus, alleviating the dissipative properties and letting the total error of the approximation tend to zero. The convergence of the approximation error to zero improves the quality of the difference schemes in the regions where the solution undergoes sharp changes. In the regions where the thermal conductivity $k(u)$ is large, the solution does not undergo sharp changes and the effect of the approximation errors is not very significant.

3.2. Numerical Analysis

Consider the formation of two fixed temperature fronts using the model heat conduction problem with boundary conditions of the first kind as an example.

To this end, we complete the quasilinear heat conduction equation (3.1) with the additional initial condition in the form of the sinusoidal half-wave

$$u^0(x, 0) = \sin(\pi x), \quad 0 < x < 1, \tag{3.10}$$

and with the homogeneous boundary conditions

$$u(0, t) = 0, \quad u(1, t) = 0. \tag{3.11}$$

We represent the nonlinear heat conduction problem (3.1), (3.10), (3.11) in terms of the variables (q, τ) by writing quasilinear equation (3.2) in the conservative form

$$\frac{\partial(\psi u)}{\partial\tau} + \frac{\partial(Qu)}{\partial q} = -\frac{\partial W}{\partial q}, \quad W = -\frac{k(u)}{\psi}\frac{\partial u}{\partial q}, \quad k(u) = k_0 u^\alpha, \quad \alpha > 1, \tag{3.12}$$

$$\frac{\partial\psi}{\partial\tau} = -\frac{\partial Q}{\partial q}, \quad \frac{\partial x}{\partial q} = \psi, \quad 0 < q < 1, \quad \tau > 0, \tag{3.13}$$

$$u^0(q, 0) = \sin(\pi q), \quad \psi(q, 0) = 1, \quad \tau = 0, \tag{3.14}$$

$$\begin{aligned} &u(0, \tau) = 0, \quad Q(0, \tau) = 0, \quad q = 0, \\ &u(1, \tau) = 0, \quad Q(1, \tau) = 0, \quad q = 1. \end{aligned} \tag{3.15}$$

In the computational space $\Omega_{q,\tau}$, we define the computational grid $\omega_h^{\Delta\tau}$ in which grid points with integer and half-integer indexes are used for convenience:

$$\omega_h^{\Delta\tau} = \{(q_i, \tau^j), (q_{i+1/2}, \tau^j):$$

$$q_{i+1} = q_i + h, q_{i+1/2} = q_i + 0.5h, i = 0, 1, \ldots, N, \tau^{j+1} = \tau^j + \Delta\tau^j, j = 0, 1, \ldots, J\}.$$

The functions x_i^j, u_i^j, and Q_i^j are defined at the integer grid points and the functions $\psi_{i+1/2}^j$ and $W_{i+1/2}^j$ are defined at the half-integer points $(q_{i+1/2}^j, \tau^j)$. Using the grid just defined, we write the following family of conservative difference schemes for the system of equations (3.12), (3.13) (see [36]):

$$\begin{aligned} (\psi\cdot u)_i^{j+1} &= (\psi\cdot u)_i^j - \frac{\Delta\tau^j}{h}\{(1-\sigma)[W_{i+1/2} - W_{i-1/2} + (u\cdot Q)_{i+1/2} - (u\cdot Q)_{i-1/2}]^j \\ &\quad + \sigma[W_{i+1/2} - W_{i-1/2} + (u\cdot Q)_{i+1/2} - (u\cdot Q)_{i-1/2}]^{j+1}\} \\ (\psi)_{i+1/2}^{j+1} &= (\psi)_{i+1/2}^j - \frac{\Delta\tau^j}{h}((1-\sigma)[Q_{i+1} - Q_i]^j + \sigma[Q_{i+1} - Q_i]^{j+1}), \\ W_{i+1/2} &= -\left(\frac{u^\alpha}{\psi}\right)_{i+1/2}\frac{u_{i+1} - u_i}{h}, \quad x_{i+1} = h\psi_{i+1/2}. \end{aligned} \tag{3.16}$$

$$Q_i = \left[\left(\frac{\alpha u^{\alpha-1}}{\psi}\right)_i \frac{1}{h}(u_{i+1/2} - u_{i-1/2}) + \frac{u_i^\alpha}{h}\left(\frac{1}{\psi_{i+1/2}} - \frac{1}{\psi_{i-1/2}}\right)\right], \quad i = 1, 2, \ldots, N-1.$$

The family of schemes (3.16) approximates the differential system with the order $O(\Delta\tau + h^2)$ for $\sigma \geq 0, 1$ and with the order $O(\Delta\tau^2 + h^2)$ for $\sigma = 0.5$. The transformation function Q determined from differential approximation (3.9) was used as the control function.

The system of nonlinear difference equations (3.16) was linearized using the iteration Newton method. At each iteration step, the system of linear algebraic equations was solved using the matrix marching. The integration step $\Delta\tau^j$ was chosen automatically on the basis of the prescribed accuracy and the maximum number of iteration steps.

The solution of differential problem (3.12)–(3.15) on a grid with $N = 21$ and $\alpha = 5$ is represented in Fig. 1 by the curves $u(t, x)$ and $\psi(t, x)$ describing the space–time distribution of the dimensionless temperature and space grid size. The number and location of the grid points in all the plots is shown by bullets (the initial distributions $u(t_0, x)$ and $\psi(t_0, x)$ for $t = t_0$), and the other curves calculated for t_1, t_2, t_3 are shown by open dots.

The curves in Fig. 1 illustrate the dynamics of formation of the fixed temperature fronts near the left and the right boundaries and the related redistribution of the grid points. Under the influence of the nonlinear conductivity, large thermal flows go from the center of the domain to the boundaries, which makes the center flatter, and regions of large gradients appear near the boundaries (the curves t_1–t_3 in Fig. 1a). The grid responds to the gradients by condensing the grid points in the regions where the gradients are large and by increasing the dimensionless size $\psi(t, x)$ in the center of the domain where the gradients of the solution are small (the curves t_1 and t_2 in Figs. 1b and 1c). The formation of the temperature fronts completes when the maximal gradients reach the boundaries. The curve $\psi(t_3, x)$ takes the same shape as $u(t_3, x)$ and remains unchanged afterwards. In the beginning of the process, the maximal grid size differed from the minimal one by several fold; by the moment when the fronts are formed, this difference reaches five orders of magnitude (the curve $\psi(t_3, x)$ in Fig. 1c). It is convenient to characterize the dynamics of the grid using the trajectories of the grid points (see Fig. 2). In the region of each of the fronts, there are only four grid points, which indicates that the total number of grid points is redundant. The calculations showed that this number might be halved without a great effect on the accuracy.

Figure 3 presents the results of the calculations for the same problem on an adapted grid with the total number of grid points $N = 11$. Note that, in order to achieve the same accuracy using a grid with fixed grid points, their number must be ~500.

The effect of the degree of nonlinearity of the thermal conductivity manifests itself in the fact that the center of the domain becomes flatter with increasing α while the fronts become steeper. Respectively, the space grid size increases in the center and decreases near the fronts even more. Figure 4 presents the space profiles of the temperature $u(x)$ and of the dimensionless grid size $\psi(x)$ computed using a grid with 10 grid points for $\alpha = 10$ at t_0, t_1, t_2, and t_3. By the time t_3, the temperature fronts are already completely formed. By this time, the dimensionless grid size decreased by five

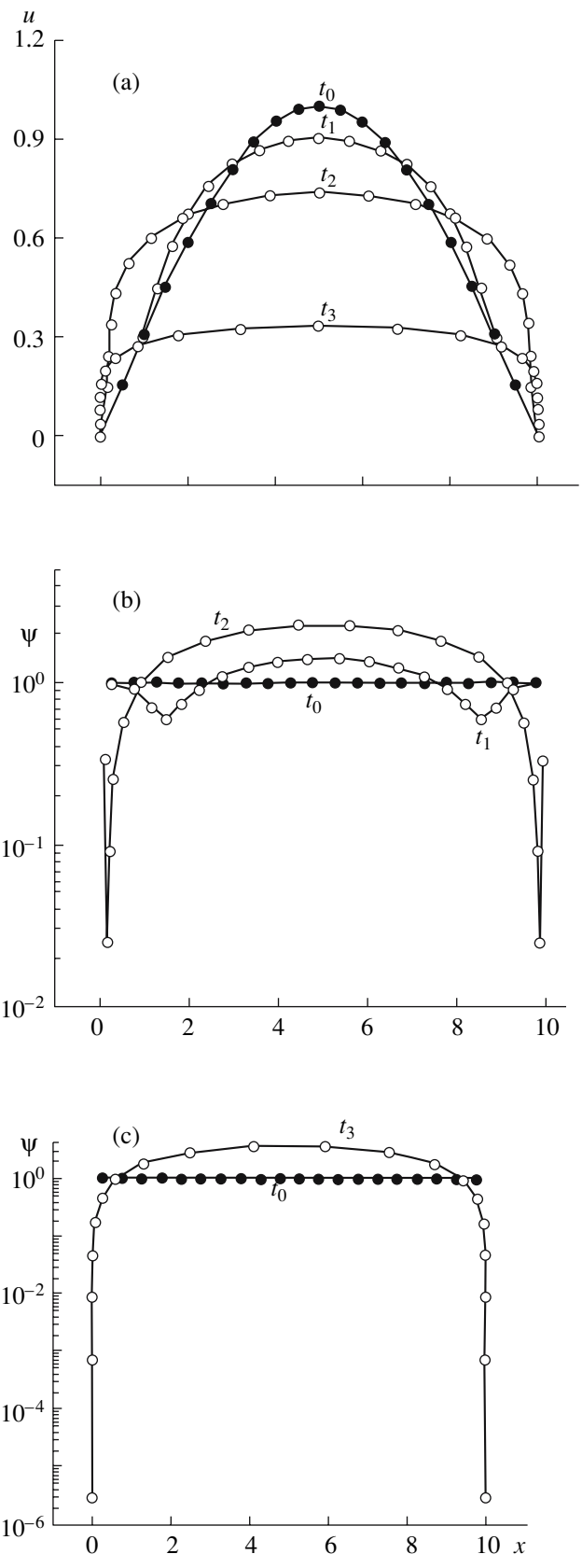

Fig. 1.

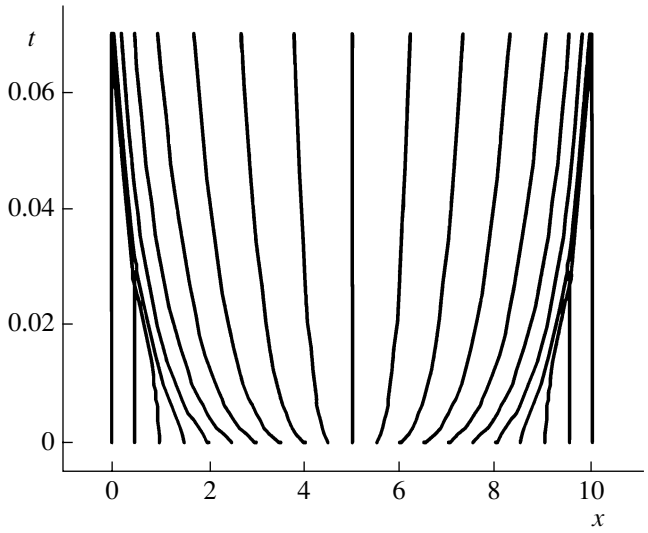

Fig. 2.

orders of magnitude near the front, while it increased by a factor of four in the center.

3.3. Propagation of Temperature Waves

Quasilinear equation (3.1) with the thermal conductivity in the form of a power function admits solutions with the derivatives that tend to infinity at the points where $u(x, t)$ vanishes and the thermal flow $W(x, t)$ is continuous; that is, $W = k(u)\dfrac{\partial u}{\partial x} \equiv 0$. In the nonlinear case, such relations lead to the appearance of a temperature front that propagates at a finite speed in the form of a temperature wave. Heat equation (3.1) supplemented with the initial and boundary conditions

$$u^0(x, 0) = 0, \quad 0 < x < \infty, \quad u(0, t) = f(t), \quad u(\infty, t) = 0, \tag{3.17}$$

admits an analytical solution in the form of a traveling wave

$$u(x, t) = \begin{cases} (\alpha D)^{1/\alpha}\{[D(t-x)]^{1/\alpha}\}, & x < Dt, \\ 0, & x \geq Dt, \end{cases} \tag{3.18}$$

where α and D are positive constants.

From the mathematical point of view, the temperature wave is the propagation of a weak discontinuity. Numerical calculations of temperature waves without tracking the weak discontinuity (see [16, 31]) showed that there is an irreducible error near the front; minimization of this error requires the use of fine grids. The situation changes drastically when the dynamic adaptation is used. Changing to an arbitrary time-dependent system of coordinates makes it possible to track the weak discontinuity in a natural way by representing the original problem as a problem with a free boundary. Tracking the weak discontinuity allows one to obtain a numerical solution with an arbitrarily small error while using the minimal number of grid points (see [18, 37]).

To track the weak discontinuity, we use the continuity equation for the flow $W(x_\Gamma(t), t) = 0$, where x_Γ is the point of the weak discontinuity. Due to the continuity of W at the point $x = x_\Gamma$, we have the equality of the fluxes on the left and on the right: $W^-(x_\Gamma(t), t) = -W^+(x_\Gamma(t), t)$. Representing $W^-(x_\Gamma(t), t)$ and $W^+(x_\Gamma(t), t)$ in the form $W^-(x_\Gamma(t), t) = v(x_\Gamma(t), t)u(x_\Gamma(t), t)$ and $W^+ = -k(u)\dfrac{\partial u}{\partial x}$, we write the condition for the discontinuity propagation velocity in the form

$$v(x_\Gamma(t), t) = -\lim_{x \to x_\Gamma(t)} \frac{W^+(x, t)}{u(x, t)} = \lim_{x \to x_\Gamma(t)} \frac{k(u(x, t))}{u(x, t)} \frac{\partial u}{\partial x}. \tag{3.19}$$

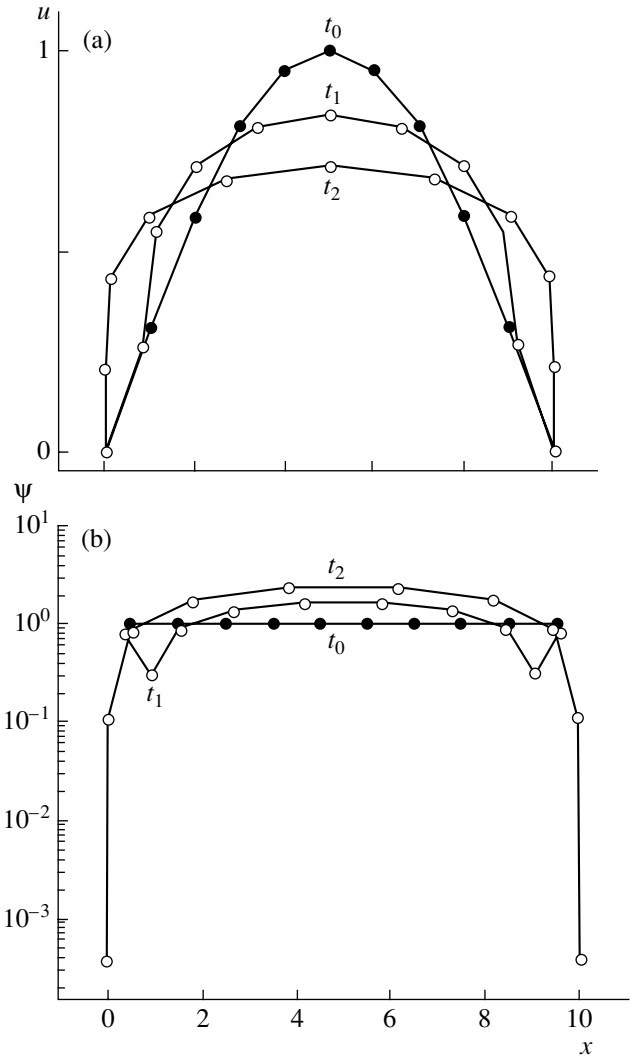

Fig. 3.

In addition to (3.19), the following condition is fulfilled at the point of discontinuity:

$$u(x_\Gamma(t), t) = 0. \tag{3.20}$$

To represent the initial problem as a problem with a free boundary, it is sufficient to bring the point of the weak discontinuity into coincidence with one of the boundaries of the interval and use (3.19) and (3.20) as boundary conditions.

In terms of the variables (q, τ), the problem of the temperature wave propagation is formulated as follows. Nonlinear differential system (3.12), (3.13) is supplemented with the boundary conditions

$$\tau = 0: \begin{cases} u^0(0, q) = 0, \\ \psi^0(0, q) = 1, \end{cases} \quad q = 0: \begin{cases} u(\tau, 0) = f(\tau), \\ Q(\tau, 0) = 0, \end{cases}$$

$$q = q_\Gamma: \begin{cases} u(\tau, q_\Gamma) = 0, \\ Q(\tau, q_\Gamma) = -v(\tau, q_\Gamma) = -\dfrac{1}{\psi}\dfrac{k(u(\tau, q_\Gamma))}{u(\tau, q_\Gamma)}\dfrac{\partial u}{\partial q} = -\dfrac{u^{\alpha-1}(\tau, q_\Gamma)}{\psi}\dfrac{\partial u}{\partial q}. \end{cases} \tag{3.21}$$

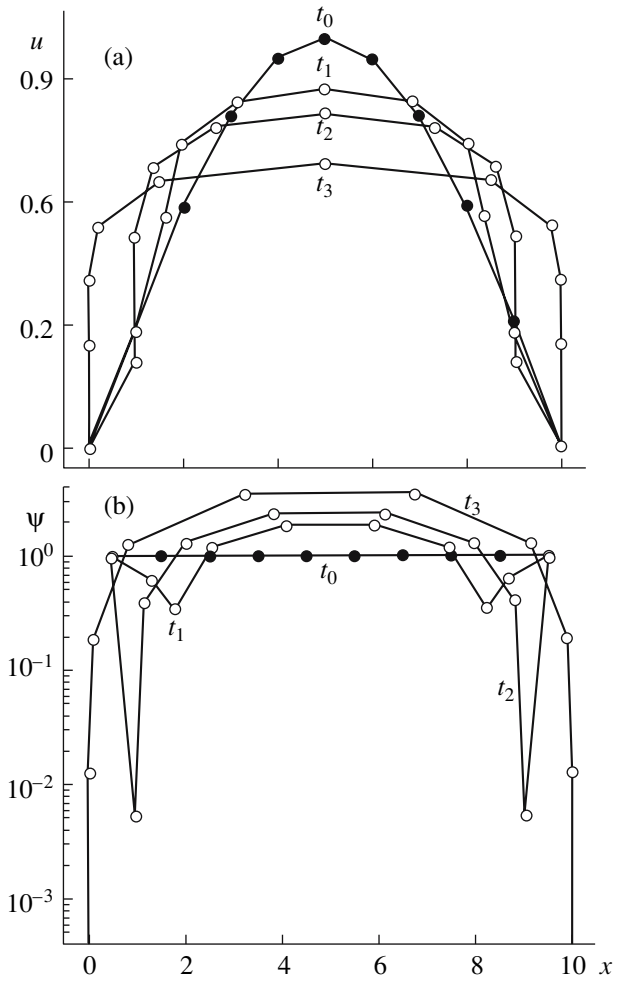

Fig. 4.

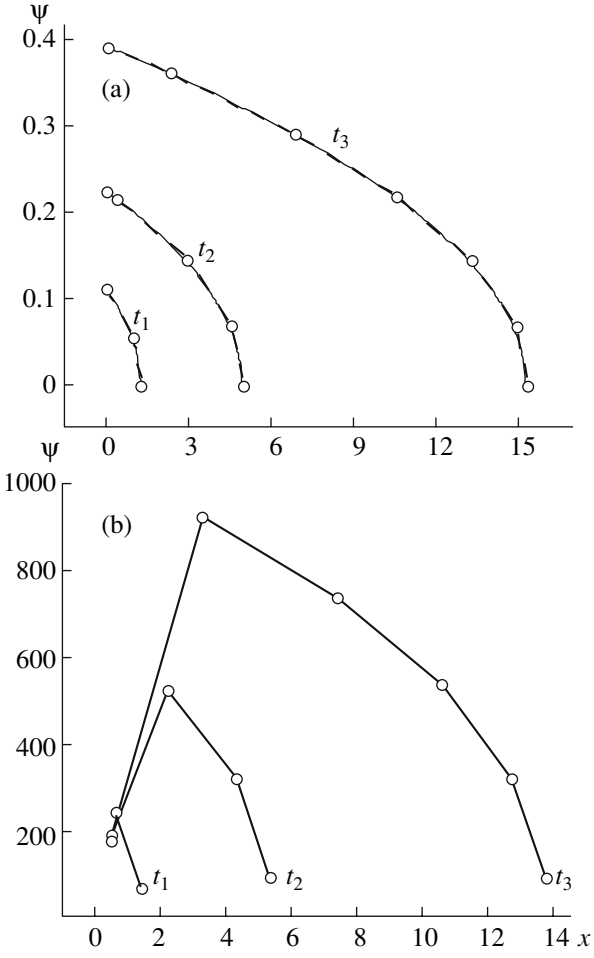

Fig. 5.

In the calculations, the following quantities were used:

$$f(\tau) = (D\alpha)^{1/\alpha}(D\tau)^{1/\alpha}, \quad D = 1, \quad \alpha = 2, 10.$$

For modeling, we used system of difference schemes (3.16). The main difference from the calculations performed earlier (see [18, 37]) is that the control function Q does not contain fitting parameters because it is determined using the principle of quasi-staionarity. The absence of fitting parameters favorably affects the accuracy of the calculations and the related number of grid points. Application of the function Q in the form of (3.9) made it possible to considerably improve the accuracy and simultaneously reduce the number of grid points by several fold compared to the results obtained in [18, 37]. The accuracy was determined by comparing the numerical solution with the analytical one. The error of the numerical solution depends on the degree of nonlinearity of the heat conductivity $k(u)$. As the parameter α grows, the degree of nonlinearity, the steepness of the front, and the error of the numerical solution also grow. For $\alpha = 2$, the curves of the analytical (dashed lines) and the numerical (solid lines) solutions coincide in Fig. 5. Some difference between the solutions appears for $\alpha \geq 10$ (see Fig. 6). In all the calculations, the number of grid points was not greater than $N \leq 10$. It turned out that so coarse a grid is sufficient even though the propagation of the wave in the problem with a free boundary expands the domain by several orders of magnitude. However, the grid must be spatially fine only in a narrow region near the front. In the other part of the domain, the spatial gradients of the solution are small; therefore, to obtain a highly accurate solution, it is sufficient to concentrate several grid points in the neighborhood of the weak discontinuity. The difference between the spatial grid sizes can be as high as several orders of magnitude, which is illustrated by the curves $\psi(x)$. For example, the ratio ψ_{max}/ψ_{min} in Fig. 6b is $\sim 10^4$.

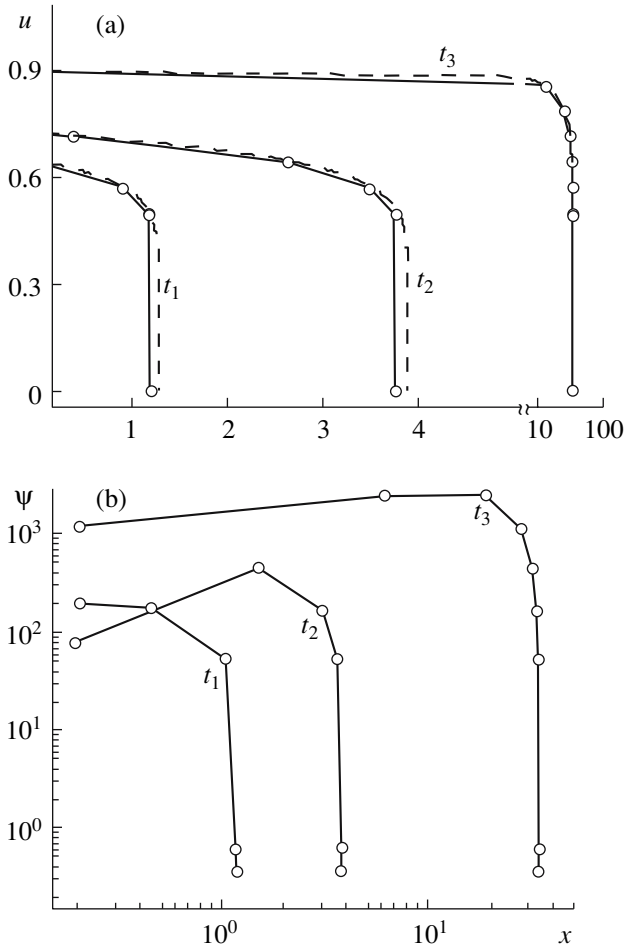

Fig. 6.

Another feature of the problem under examination is that it belongs to the class of problems in which calculations on grids with a variable number of nodes are especially effective. Since the domain of the solution significantly expands, it is not reasonable to use a grid with a large number of nodes at the beginning of the calculations when the size of the domain is still small. In the examples considered in this paper, the initial grid contained only $N = 3$ nodes. As the domain expands, new nodes were generated near the left boundary (see Figs. 5, 6).

The results of the computations show that the dynamic adaptation method is very efficient in nonlinear heat conduction problems.

The analysis of the differential approximation and numerical solution shows that the dynamic adaptation method based on the principle of quasi-staionarity significantly improves the quality of finite difference schemes. The grid refinement in the region of large gradients fitted to the solution reduces the scheme viscosity and eliminates the variation of the scheme almost completely.

4. NONLINEAR CONVECTION-DIFFUSION EQUATIONS (BUCKLEY–LEVERETTE AND BURGERS EQUATIONS)

The use of relations (1.6) in Eq. (1.1) leads to the parabolic Buckley–Leverette equation, which is the main equation in the model problem describing the motion of a two-phase immiscible fluid (for example, oil–water) in a porous medium; this model describes the convective transport and diffusion.

Application of relations (1.5) turns Eq. (1.1) into the complete Burgers equation, which provides a model for the boundary layer equations, the Navier–Stokes equations brought to the parabolic form, and the complete Navier–Stokes equations (see [38]).

4.1. Statement of the Problem

Both equations have the same structure and differ only by the form of the nonlinear operator $P(u)$:

$$\frac{\partial u}{\partial t} + \frac{\partial P(u)}{\partial x} = \frac{\partial}{\partial x}\mu\frac{\partial u}{\partial x}, \quad x_0 < x < \infty, \quad t > 0. \tag{4.1}$$

Here, $P(u) = \dfrac{u^2}{u^2 + \alpha(1-u)^2}$ for the Buckley–Leverette equation, $P(u) = \dfrac{u^2}{2}$ for the Burgers equation, and $\mu \sim \mathrm{Re}^{-1} \ll 1$ (the small parameter multiplying the higher order derivative) is interpreted as diffusion in the Buckley–Leverette equation and as viscosity in the Burgers equation. Due to the small multiplier of the higher order derivative, both equations belong to the class of singularly perturbed equations. The solution to such equations is complicated because regions of the sharp variation of the solution may appear under some boundary conditions. The difference schemes used to solve convection–diffusion equations in the case when convection is prevailing usually have large variation, which results in the appearance of parasitic oscillations when the solution changes in a jump. We demonstrate the efficiency of the dynamic adaptation method for solving equations of this class.

Using the change of variables of the general form and relations (2.1), we rewrite Eq. (4.1) in terms of the variables (q, τ):

$$\frac{\partial u}{\partial \tau} + \frac{Q}{\psi}\frac{\partial u}{\partial q} + \frac{1}{\psi}\frac{\partial P(u)}{\partial q} = \frac{1}{\psi}\frac{\partial}{\partial q}\frac{\mu}{\psi}\left(\frac{\partial u}{\partial q}\right), \tag{4.2}$$

$$\frac{\partial \psi}{\partial \tau} = -\frac{\partial Q}{\partial q}, \quad \psi = \frac{\partial x}{\partial q}, \quad q_0 < q < q_R, \quad \tau > 0. \tag{4.3}$$

The quasi-stationarity condition $\partial u/\partial\tau = 0$ yields the following equation from which the function Q can be determined:

$$Q\frac{\partial u}{\partial q} + \frac{\partial P(u)}{\partial q} - \frac{\partial}{\partial q}\left(\frac{\mu}{\psi}\frac{\partial u}{\partial q}\right) = 0, \tag{4.4}$$

$$Q = -\left(\frac{\partial P(u)}{\partial u} - \frac{\partial}{\partial q}\left(\frac{\mu}{\psi}\right) - \frac{\mu}{\psi}\frac{\partial^2 u}{\partial q^2}\Big/\frac{\partial u}{\partial q}\right). \tag{4.5}$$

Here, $\dfrac{\partial P(u)}{\partial u}$ has the form

$$\frac{\partial P(u)}{\partial u} = \frac{2\alpha u(1-u)}{[u^2 + \alpha(1-u)^2]^2}, \quad \frac{\partial P(u)}{\partial u} = u$$

for the Buckley–Leverette and Burgers equations, respectively.

4.2. Analysis of the Differential Approximations

In the discrete space $\omega_h^{\Delta\tau}$, consider the family of five-point schemes for time-independent equation (4.4). The analytical investigation of the quality of these schemes is much easier than the investigation of the schemes for time-dependent equation (4.2). The scheme with the central difference quotients has the form

$$Q_i\frac{u_{i+1} - u_{i-1}}{2h} + \frac{P_{i+1} - P_{i-1}}{2h} - \frac{1}{h}\left(\frac{\mu}{\Psi_{i+1/2}}\frac{u_{i+1} - u_i}{h} - \frac{\mu}{\Psi_{i-1/2}}\frac{u_i - u_{i-1}}{h}\right) = 0, \tag{4.6}$$

the scheme based on the forward difference quotients is

$$Q_i\frac{u_{i+1} - u_i}{h} + \frac{P_{i+1} - P_i}{h} - \frac{1}{h}\left(\frac{\mu}{\Psi_{i+1/2}}\frac{u_{i+1} - u_i}{h} - \frac{\mu}{\Psi_{i-1/2}}\frac{u_i - u_{i-1}}{h}\right) = 0, \tag{4.7}$$

and the scheme based on the backward difference quotients is

$$Q_i\frac{u_i-u_{i-1}}{h}+\frac{P_i-P_{i-1}}{h}-\frac{1}{h}\left(\frac{\mu}{\Psi_{i+1/2}}\frac{u_{i+1}-u_i}{h}-\frac{\mu}{\Psi_{i-1/2}}\frac{u_i-u_{i-1}}{h}\right)=0. \tag{4.8}$$

For schemes (4.6)–(4.8), we write their differential approximations, which differ only by the coefficients on the right-hand sides:

$$Q\frac{\partial u}{\partial q}-\frac{\partial}{\partial q}\left(\frac{\mu}{\psi}\frac{\partial u}{\partial q}\right)=\delta_n\frac{\partial u}{\partial q}+\alpha_n\frac{\partial^2 u}{\partial q^2}+\beta_n\frac{\partial^3 u}{\partial q^3}+\gamma_n\frac{\partial^4 u}{\partial q^4},\quad n=1,2,3. \tag{4.9}$$

For scheme (4.6) based on the central difference quotients ($n=1$), we have

$$\delta_1=-\frac{h^2}{24}\left(\left(4\frac{\partial^3 P}{\partial u^3}\right)\left(\frac{\partial u}{\partial q}\right)^2-\frac{\partial^3}{\partial q^3}\left(\frac{\mu}{\psi}\right)\right),\quad \alpha_1=-\frac{h^2}{8}\left(4\frac{\partial^2 P}{\partial u^2}\frac{\partial u}{\partial q}-\frac{\partial^2}{\partial q^2}\left(\frac{\mu}{\psi}\right)\right),$$

$$\beta_1=-\frac{h^2}{6}\left(Q+\frac{\partial P}{\partial u}-\frac{\partial}{\partial q}\left(\frac{\mu}{\psi}\right)\right),\quad \gamma_1=\frac{h^2}{12}\frac{\mu}{\psi}.$$

For the schemes with the forward difference quotients (4.7) ($n=2$) and backward quotients ($n=3$), the differential approximations differ only by the sign on the right-hand side:

$$Q\frac{\partial u}{\partial q}+\frac{\partial P(u)}{\partial q}-\frac{\partial}{\partial q}\frac{\mu}{\psi}\frac{\partial u}{\partial q}=\delta_{2,3}\frac{\partial u}{\partial q}+\alpha_{2,3}\frac{\partial^2 u}{\partial q^2}+\beta_{2,3}\frac{\partial^3 u}{\partial q^3}+\gamma_{2,3}\frac{\partial^4 u}{\partial q^4}. \tag{4.10}$$

Here, $\delta_{2,3}=\delta_1+\delta_0$, $\alpha_{2,3}=\alpha_0+\alpha_1$, $\beta_{2,3}=\beta_1$, $\gamma_{2,3}=\gamma_1$,

$$\delta_0=\mp\frac{h}{2}\frac{\partial^2 P}{\partial u^2}\frac{\partial u}{\partial q},\quad \alpha_0=\mp\frac{h}{2}\left(Q+\frac{\partial P}{\partial u}\right).$$

Here, the index 2 corresponds to the equation for scheme (4.7), and the index 3 corresponds to the differential approximation for scheme (4.8). The upper sign in $\delta_{2,3}$ and $\alpha_{2,3}$ corresponds to the index 2, and the lower sign to the index 3.

Let us analyze the coefficients α and β multiplying the second-order and the third-order derivatives; they characterize, respectively, the dissipation and the variation of difference schemes. Both coefficients depend on the adaptation parameter, which indicates that the dissipation and variation of the schemes depend on the adaptation method, and an appropriate choice of the control function Q can increase or decrease the dissipation and variation. The coefficient β has the same form for all three families of schemes; it vanishes if Q is chosen as

$$Q=-\left(\frac{\partial P}{\partial u}-\frac{\partial}{\partial q}\left(\frac{\mu}{\psi}\right)\right). \tag{4.11}$$

Expression (4.11) is shorter by one term than (4.3), and it allows us to completely eliminate the internal variation of the schemes.

Scheme (4.6) based on the central difference quotients has the minimal variation among the three schemes under examination. In the corresponding differential approximation (4.9), the coefficient of the dissipative term α_1 is proportional to h^2. Taking into account the choice of Q in form (4.11), scheme (4.6) is formally the best one: it has a small scheme viscosity and no variation. In the second-order difference schemes with fixed grid points for convection–diffusion equations, small dissipation plays a negative role because a small scheme viscosity cannot suppress parasitic oscillations of the solution since the dispersive component is not compensated for. In schemes (4.7) and (4.8) of the first order $O(h)$, the dispersive component is proportional to h and $\alpha_{2,3}\approx h$. However, the scheme viscosity is not large in this case and does not play as significant a role as in schemes with fixed grid points. The coefficients α_2 and α_3 in Eq. (4.10) are a sum of $\alpha_1\sim h^2$ and an addition $\alpha_0=\mp\frac{h}{2}\left(Q+\frac{\partial P}{\partial u}\right)$, which depends on the transformation function Q. When

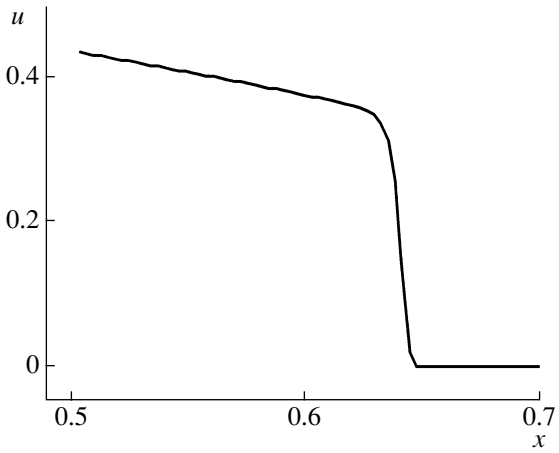

Fig. 7.

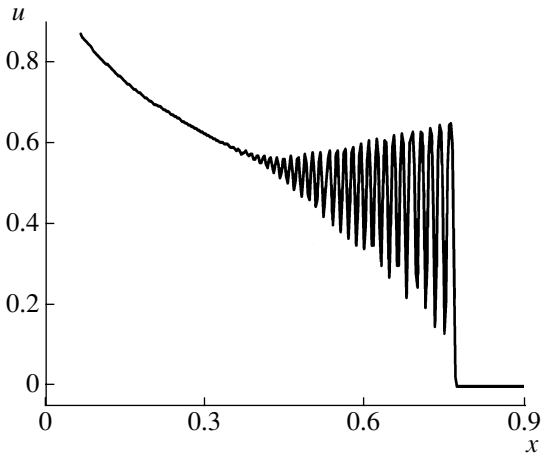

Fig. 8.

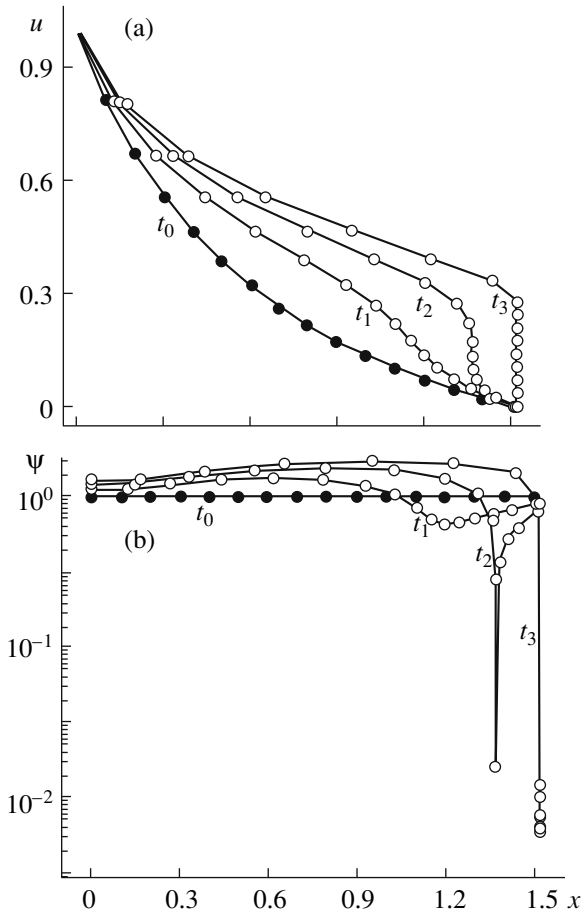

Fig. 9.

Q is given by (4.11), i.e., is proportional to the diffusion or viscosity coefficient μ, we have

$$\alpha_0 = \mp\frac{h}{2}\frac{\partial}{\partial q}\left(\frac{\mu}{\psi}\right).$$

In the most interesting cases when μ is very small, α_0 is vanishingly small and the quality of schemes (4.7) and (4.8) is similar to scheme (4.6). For large μ, the scheme viscosity is of little importance because large diffusion or viscosity prevents the formation of steep gradients of the solution.

Thus, the analysis of the differential approximation shows that, as in nonlinear heat conduction problems, the dynamic adaptation considerably improves the quality of the difference schemes. The grid refinement in the region where the gradients are large reduces the scheme viscosity and practically eliminates the variation of the difference schemes.

The differential approximation can be also used to determine the optimal transformation function Q because the results are close to those obtained using the principle of quasi-stationarity.

4.3. Numerical Solution of Model Problems

Consider two typical statements of convection–diffusion problems that use the Buckley–Leverette equation (see [39]) and Burgers equations.

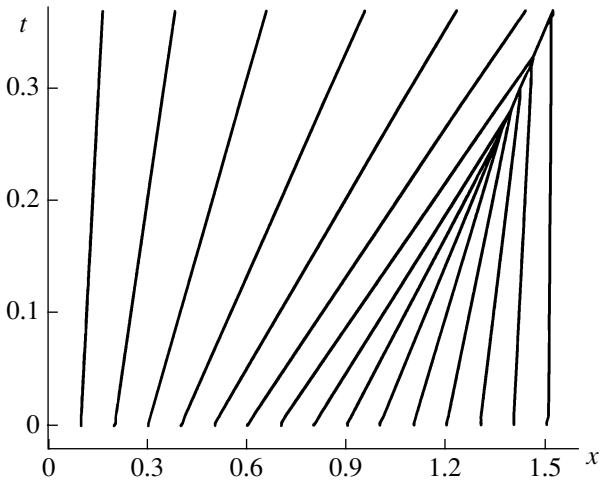

Fig. 10.

4.3.1. Buckley–Leverette equation. Define $W(u) = P(u) - \mu\dfrac{\partial u}{\partial x}$, and write the Buckley–Leverette equations in terms of the variables (q, τ) in the conservative form

$$\frac{\partial(\psi u)}{\partial t} = -\frac{\partial(Q\cdot u)}{\partial q} - \frac{\partial W}{\partial q}, \tag{4.12}$$

$$\frac{\partial \psi}{\partial t} = -\frac{\partial Q}{\partial q}, \quad q_0 < q < q_\infty, \quad \tau > 0, \tag{4.13}$$

where

$$P(u) = \frac{u^2}{u^2 + \alpha(1-u)^2}, \quad Q(u) = -\left\{\frac{2\alpha u(1-u)}{[u^2 + \alpha(1-u)^2]^2} - \frac{\mu}{\psi}\frac{\partial u}{\partial q}\right\},$$

subject to the initial and boundary conditions

$$\tau = 0: \begin{cases} u(0,q) = u^0(q), \\ \psi(0,q) = \psi^0(q), \end{cases} \quad q = 0: \begin{cases} u(\tau,0) = g_0(t), \\ Q(\tau,0) = 0, \end{cases} \quad q = \infty: \begin{cases} u(\tau,\infty) = g_\infty(\tau), \\ Q(\tau,\infty) = 0, \end{cases} \tag{4.14}$$

where u characterizes the saturation by the fluid, μ has the sense of the diffusion coefficient, α is the parameter characterizing the mobility of one fluid relative to the other, and $u^0(q)$, $\psi^0(q)$, $g_0(\tau)$, and $g_\infty(\tau)$ are known functions.

The representation of the Buckley–Leverette equation in form (4.12) makes it possible to use, for the numerical solution, the family of implicit conservative difference schemes (3.16). In this case, the quantities $Q(u)$ and $W(u)$ are approximated by the finite difference relations

$$W_{i+1/2} = \left(\frac{u^2}{(u^2 + \alpha(1-u)^2)}\right)_{i+1/2} - \left(\frac{\mu}{\psi}\right)_{i+1/2}\frac{u_{i+1} - u_i}{h}, \tag{4.15}$$

$$Q_i = -\left[\left(\frac{2\alpha u(1-u)}{[u^2 + \alpha(1-u)^2]^2}\right)_i - \frac{\mu}{h}\left(\frac{1}{\psi_{i+1/2}} - \frac{1}{\psi_{i-1/2}}\right)\right]. \tag{4.16}$$

In the calculations, we used the following values of the functions and parameters:

$$u^0(q) = e^{-10q}, \quad \psi^0(q) = 1, \quad g_0(\tau) = 1, \quad g_\infty(\tau) = 0, \quad \mu = 10^{-5}, \quad \alpha = 0.25, 2.5. \tag{4.17}$$

4.3.2. Modeling results. First, for comparison, we solved Eq. (4.1) subject to conditions (4.17) on a grid with $N = 500$ fixed nodes. The results obtained using schemes of the first order $O(\Delta\tau + h^2)$ and of the second

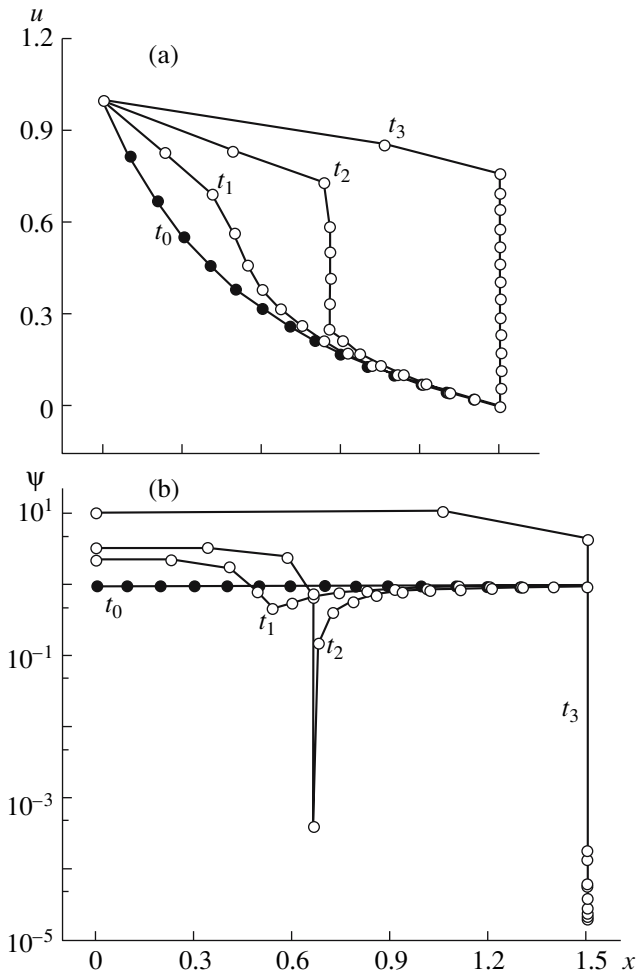

Fig. 11.

order $O(\Delta\tau^2 + h^2)$ are presented in Figs. 7 and 8. Schemes of the first order yield a solution that is significantly smoothed near the front (Fig. 7) and schemes of the second order yield a poor solution due to a large variation (Fig. 8).

Application of dynamically adapted grids for solving problem (4.12)–(4.14), (4.17) using difference schemes (3.16), (4.15), (4.16) of the first and second orders makes it possible to obtain solutions that are not smoothed and have no parasitic oscillations using only 10–20 grid points. Figure 9 shows the spatial distribution of the function $u(x)$ and the distribution of the dimensionless grid size $\psi(x)$ for various moments of time for $\alpha = 0.25$, $\mu = 10^{-5}$, and $N = 16$.

Strong nonlinearity of the equation in combination with slow diffusion promotes the formation of large gradients in the interior of the domain, which affect the redistribution of the grid points. In a short period of time, the space grid size near the nonlinear front reduces by three orders of magnitude, while it increases by a factor of ~25 in the region of the slow variation of the solution. The dynamics of the grid points is characterized by their trajectories (see Fig. 10). Nine grid points of the total number of $N = 16$ points are concentrated on the front.

The coefficient α is the nonlinearity parameter; its value determines the location and time of the front formation. When $\alpha = 0$, Eq. (4.1) is linear, the solution has no fronts, and the grid points remain fixed. When α increases, the region of the nonlinear front formation shifts to the left and its amplitude increases. Correspondingly, more grid points

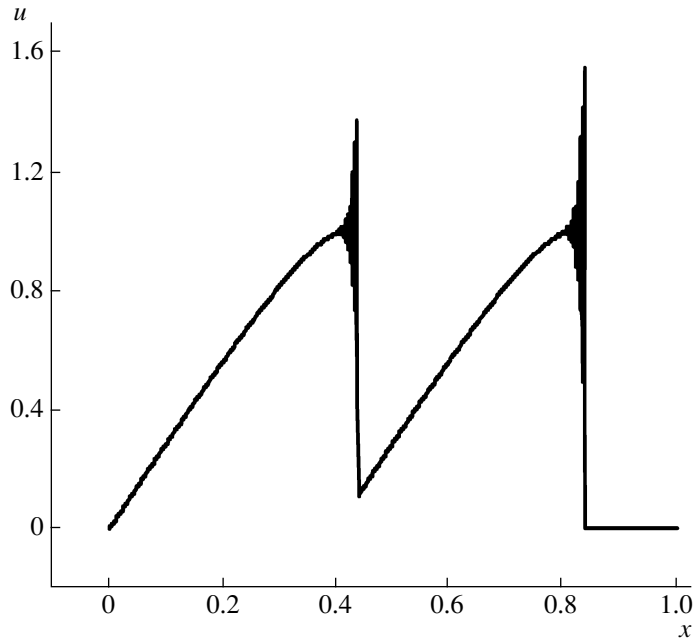

Fig. 12.

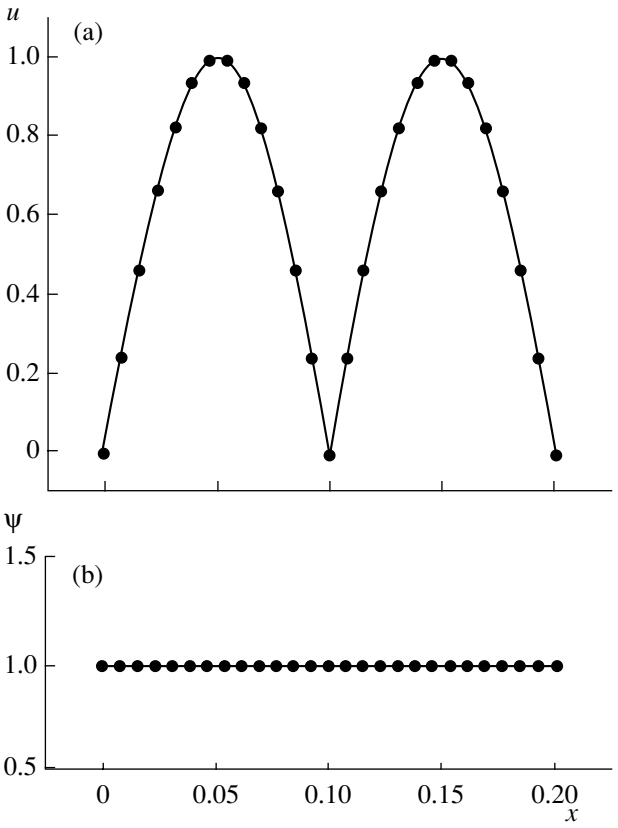

Fig. 13.

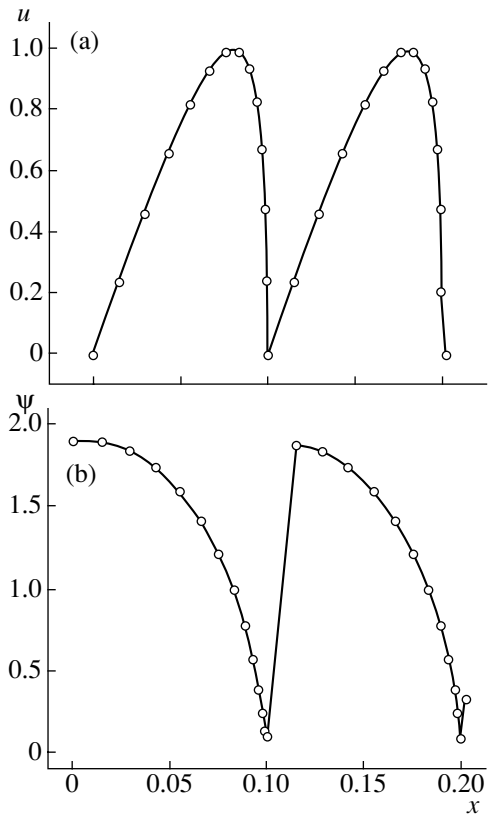

Fig. 14.

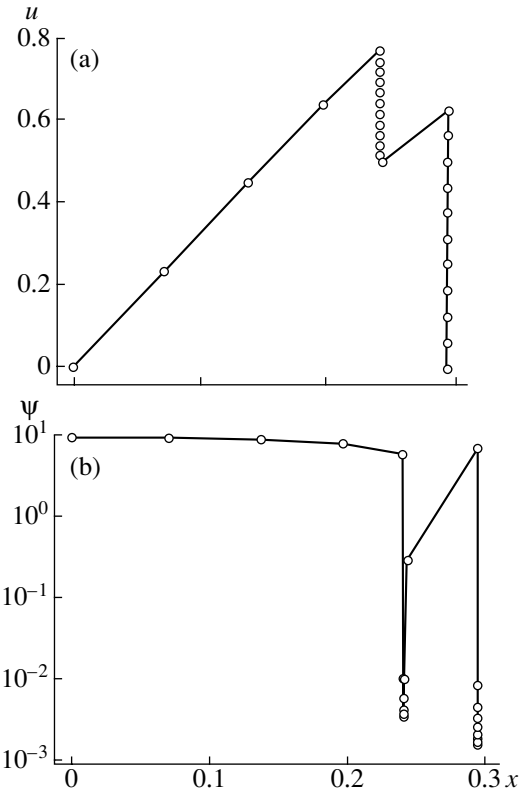

Fig. 15.

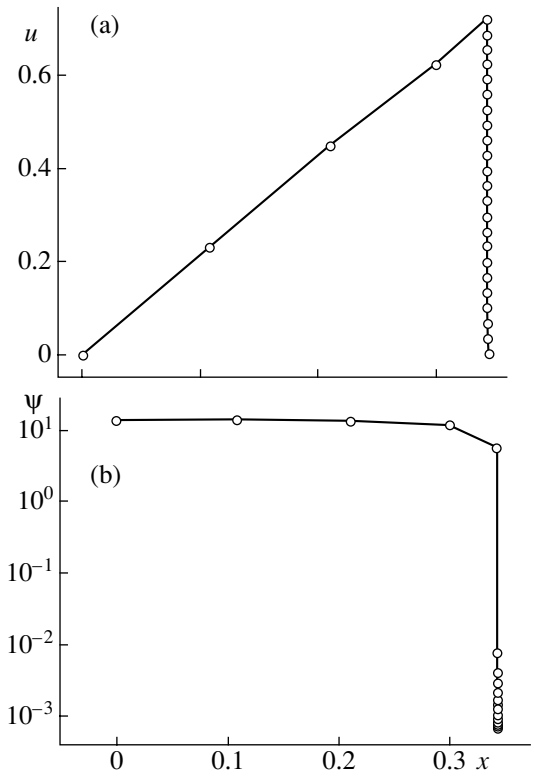

Fig. 16.

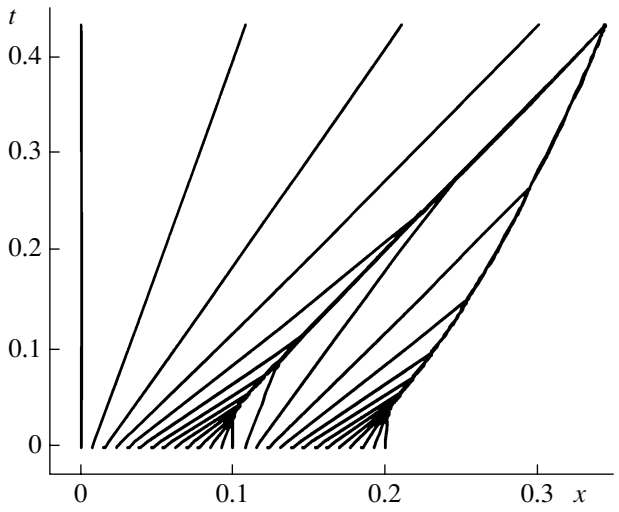

Fig. 17.

are concentrated near the front. The dynamics of the solution and of the grid points for $\alpha = 2.5$ is illustrated in Fig. 11.

4.3.3. Burgers equation. The complete Burgers equation provides a model for the behavior of nonlinear waves, which typically contain one or several steep fronts. The complexity of finding numerical solutions of model Burgers problems is well known (e.g., see [39, 40]).

In terms of the variables (x, t), the Burgers equation has the form

$$\frac{\partial u}{\partial t} + \frac{\partial (u^2/2)}{\partial x} = \frac{\partial}{\partial x}\mu\frac{\partial u}{\partial x}, \quad x_0 < x < x_\infty, \quad t > 0. \tag{4.18}$$

Consider the typical statement of the problem in which the solution to the Burgers equation tends to a discontinuous solution because the physical viscosity $\mu = 10^{-5}$ is small. Due to a special choice of the initial space profile $u^0(x)$, the quasi-discontinuous solution appears in the middle of the domain and on its boundary.

The initial distribution $u(x, 0)$ was represented by two positive sinusoidal half-waves

$$u(x, 0) = u^0(x) = \begin{cases} |\sin(2\pi x/x_R)|, & 0 < x < x_R, \\ 0, & x > x_R. \end{cases} \tag{4.19}$$

The boundary conditions were chosen in the form

$$u(x_0, t) = u(x_R, t) = 0. \tag{4.20}$$

Representing the function $W(u)$ in the form $W(u) = \dfrac{u^2}{2} - \mu\dfrac{\partial u}{\partial x}$, the Burgers equation in the variables (q, τ) is reduced to system (4.12), (4.13), which allows us to use the family of difference schemes (3.16) complemented with the finite difference relations

$$W_{i+1/2} = \frac{u_{i+1/2}^2}{2} - \frac{\mu}{\psi_{i+1/2}}\frac{u_{i+1} - u_i}{h}, \quad Q_i = -\left[u_i - \frac{\mu}{h}\left(\frac{1}{\psi_{i+1/2}} - \frac{1}{\psi_{i-1/2}}\right)\right]. \tag{4.21}$$

4.3.4. Modeling results. Under the influence of the convective component and small physical viscosity $\mu = 10^{-5}$, the solution tends to a discontinuous solution as time increases.

First, problem (4.18)–(4.20) was solved on the grid with the total number of $N = 2000$ fixed nodes. Due to a special choice of the initial space distribution $u^0(x)$, two quasi-discontinuous solutions appear in the interior of the domain. When the second-order difference scheme is used, parasitic oscillations appear near both fronts, which cannot be gotten rid of even with $N = 5000$ (see Fig. 12).

Figures 13–17 illustrate the solution of problem (4.12), (4.13), (4.19), (4.20) obtained at various moments of time using a dynamically adapted grid with the total number of grid points $N = 25$. The calculations were performed using second-order scheme (4.21). Figure 13 shows the initial distribution of the functions $\psi(t_0, x)$ and $u(t_0, x)$. The calculations showed that, in a short period of time, a quasi-discontinuous solution appears in each of the half-waves. The grid responds to the appearance of large gradients by increasing the number of nodes in the neighborhood of the right boundaries of the half sinusoids (the curves $\psi(t, x)$ and $u(t, x)$ in Fig. 14). By the time when two fronts begin to form, the grid size decreases by several orders of magnitude. With time, the left front catches up with the right front (the curves $\psi(t, x)$ and $u(t, x)$ in Fig. 15), and then it absorbs the right front (the curves $\psi(t, x)$ and $u(t, x)$ in Fig. 16). Later, the triangular shape remains along with the propagation in the mode with a single front (see the curves in Fig. 15). The major part of the grid points concentrate on the front of the solution. The dynamics of the front formation and their merging are best seen in the diagram of the node motion (see Fig. 17).

The complete absence of oscillations is achieved due the relocation of nodes fitted to the solution; as a result, the variation of the schemes completely vanishes. Due to this property of the difference schemes written in time-dependent systems of coordinates, dynamically adapted grids require an unusually small number of grid points.

CONCLUSIONS

In this paper, we performed a detailed analysis of the capabilities of the dynamic adaptation method as applied to the numerical solution to parabolic partial differential equations. A generalization of the results obtained for the nonlinear heat conduction and convection–diffusion equations shows that the idea of using the unknown solution for generating adapted grids makes the dynamic adaptation method universal, efficient, and algorithmically simple.

Universality is ensured by the use of an arbitrary time-dependent system of coordinates whose velocity depends on and is determined by the unknown solution.

The efficiency is ensured by automatically fitting the velocity of the grid point motion to the dynamics of the solution.

This is achieved using the optimal transformation function. The components of the contracting and repulsive actions are contained in the original equation itself, and they are introduced in the control function using the principle of quasi-stationarity. The close relationship of the adaptation mechanism with the structure of the parabolic equation makes it possible to perform an automatic control of the grid points relocation, thus, preventing their trajectories from intersecting. This mechanism is inherent in all parabolic equations in contrast to the hyperbolic equations whose structure does not contain repulsive components. Dynamically adapted grids for hyperbolic equations admit the intersection of the trajectories of the grid points. To avoid this effect, the repulsive components are artificially introduced into the control function.

The algorithmic simplicity is achieved by a universal approach to the generation of adapted grids independently of the type of the differential equation.

ACKNOWLEDGMENTS

This work was supported by the Russian Foundation for Basic Research, project nos. 06-07-89191 and 07-07-00045.

REFERENCES

1. J. F. Thompson, Z. U. A. Warsi, and C. W. Mastin, "Boundary-Fitted Coordinate Systems for Numerical Solution to Partial Differential Equations. A Review," J. Comput. Phys. **47** (1), 1–108 (1982).
2. J. F. Thompson, Z. U. A. Warsi, and C. W. Mastin, *Numerical Grid Generation: Foundations and Applications* (North-Holland, New York, 1985).
3. *Modeling, Mesh Generation, and Adaptive Numerical Methods for Partial Differential Equations*, Ed. by I. Babuska, J. E. Flaherty, W. D. Henshaw, J. E. Hopcroft (Springer, New York, 1995).
4. *Proceedings of the 4th–9th International Conferences on Numerical Grid Generation in Computational Field Simulations*, 1994–2005.
5. *Applied Geometry, Grid Generation, and Highly Accurate Computations, Trudy Vserossiiskoi Konferentsii,* Ed. by Yu. G. Evtushenko, M. K. Kerimov, and V. A. Garanzha (Vychisl. Tsentr Ross. Akad. Nauk, Moscow, 2004), Vol. 1 [in Russian].

6. J. U. Brackbill and J. Saltzman, "Adaptive Zoning for Singular Problems in Two Dimensions," J. Comput. Phys. **46**, 342–368 (1982).
7. D. A. Anderson, "Equidistribution Schemes, Poisson Generators, and Adaptive Grids," Appl. Math. Comput. **24**, 211–227 (1987).
8. K. Matsuno and H. A. Dwyer, "Adaptive Methods for Elliptic Grid Generation," J. Comput. Phys. **77**, 40–52 (1988).
9. S. A. Ivanenko and G. P. Prokopov, "Methods of Adaptive Harmonic Grid Generation," Zh. Vychisl. Mat. Mat. Fiz. **37**, 643–662 (1997) [Comput. Math. Math. Phys. **37**, 627–645 (1997)].
10. M. J. Berger and P. Colella, "Local Adaptive Mesh Refinement for Shock Hydrodynamics," J. Comput. Phys. **82**, 64–84 (1989).
11. M. J. Berger, "Data Structures for Adaptive Grid Generation," SIAM J. Sci. Statist. Comput. **3**, 904–916 (1986).
12. J. M. Hyman and S. Li, *Iterative and Dynamic Control of Adaptive Mesh Refinement with Nested Hierarchical Grids* (Los Alamos Lab., 1998) Report No. 5462.
13. A. Andersen, X. Zheng, and V. Cristini, "Adaptive Unstructured Volume Remeshing. I: The Method," J. Comput. Phys. **208**, 616–625 (2005).
14. R. R. Nourgaliev, T. N. Dinh, and T. G. Theofanous, "Adaptive Characteristics-Based Matching for Compressible Multifluid Dynamics," J. Comput. Phys. **213** (2), 500–529 (2006).
15. N. A. Dar'in and V. I. Mazhukin, "An Approach to Generation of Adaptive Grids," Dokl. Akad. Nauk SSSR **298**, 64–68 (1988).
16. N. A. Dar'in and V. I. Mazhukin, "An Approach to the Generation of Adaptive Grids for Nonstationary Problems," Zh. Vychisl. Mat. Mat. Fiz. **28**, 454–460 (1988).
17. N. A. Dar'in, V. I. Mazhukin, and A. A. Samarskii, "A Finite Difference Method for Solving One-Dimensional Gas Dynamics Problems on Adaptive Grids," Dokl. Akad. Nauk SSSR **302**, 1078–1081 (1988).
18. V. I. Mazhukin and L. Yu. Takoeva, "Principles of Generation of Dynamic Grids That Adapt to Solutions of One-Dimensional Boundary Value Problems," Mat. Modelir. **2** (3), 101–118 (1990).
19. V. I. Mazhukin, A. A. Samarskii, O. Kastel'yanos, and A. V. Shapranov, "The Dynamic Adaptation Method for Nonstationary Problems with High Gradients," Mat. Modelir. **5** (4), 32–56 (1993).
20. P. V. Breslavskii and V. I. Mazhukni, "The Dynamic Adaptation Method in Gas Dynamics," Mat. Modelir. **7** (12), 48–78 (1995).
21. W. H. Hui, P. Y. Li, and Z. W. Li, "A Unified Coordinate System for Solving the Two-Dimensional Euler Equations," J. Comput. Phys. **153**, 596–637 (1999).
22. W. H. Hui and S. Kudriakov, "A Unified Coordinate System for Solving the Three-Dimensional Euler Equations," J. Comput. Phys. **172**, 235–260 (2001).
23. A. N. Gil'manov, "Application of Dynamically Adaptive Grids to the Analysis of Flows with a Multiscale Structure," Zh. Vychisl. Mat. Mat. Fiz. **41**, 311–326 (2001) [Comput. Math. Math. Phys. **41**, 289–303 (2001)].
24. D. V. Rudenko and S. V. Utyuzhnikov, "Use of Dynamically Adaptive Grids for Modeling Three-Dimensional Unsteady Gas Flows with High Gradients," Zh. Vychisl. Mat. Mat. Fiz. **42**, 395–409 (2002) [Comput. Math. Math. Phys. **42**, 377–390 (2002)].
25. H. Tang and T. Tang, "Adaptive Mesh Methods for One- and Two-Dimensional Hyperbolic Conservation Laws," SIAM J. Numer. Anal. **41**, 487–515 (2003).
26. P. V. Breslavskii and V. I. Mazhukin, "Dynamically Adapted Grids for Interacting Discontinuous Solutions," Zh. Vychisl. Mat. Mat. Fiz. **47**, 717–737 (2007) [Comput. Math. Math. Phys. **47**, 687–706 (2007)].
27. M. M. Demin, V. I. Mazhukin, and A. A. Shapranov, "Dynamic Adaptation Method for a Laminar Combustion Problem," Zh. Vychisl. Mat. Mat. Fiz. **41**, 648–661 (2001) [Comput. Math. Math. Phys. **41**, 609–621 (2001)].
28. M. M. Demin, A. V. Shapranov, and I. Smurov, "The Method of Construction Dynamically Adapting Grids for Problems of Unstable Laminar Combustion," Numer. Heat Transfer. Part B: Fundamentals **44**, 387–415 (2003).
29. A. V. Lykov, *Theory of Heat Conduction* (Vysshaya Shkola, Moscow, 1967) [in Russian].
30. Ya. B. Zel'dovich and A. S. Kompaneets, "On the Theory of Heat Propagation in the Case when the Thermal Conductivity Depends on Temperature," in *On the 70th Anniversary of the Birth of A. F. Ioffe* (Akad. Nauk SSSR, Moscow, 1950), pp. 61–71 [in Russian].
31. A. A. Samarskii and I. M. Sobol', "Examples of Numerical Calculation of Temperature Waves," Zh. Vychisl. Mat. Mat. Fiz. **3**, 702–719 (1963).
32. P. P. Volosevich and E. I. Levanov, *Self-Similar Solutions in Gas Dynamics and Heat Transfer* (Moscow Inst. For Physics and Technology, Moscow, 1997) [in Russian].
33. G. I. Barenblatt and M. I. Vishik, "On Finite Rate of Propagation in Problems of Nonstationary Filtration of Fluids," Prikl. Mat. Mekh. **20**, 411–417 (1956).

34. R. E. Warming and B. J. Hyett, "The Modified Equation Approach to the Stability and Accuracy Analysis of Finite-Difference Methods," J. Comput. Phys. **14**, 159–179 (1974).

35. Yu. I. Shokin, *First Differential Approximation* (Nauka, Novosibirsk, 1979) [in Russian].

36. A. A. Samarskii, *Theory of Finite Difference Schemes* (Nauka, Moscow, 1989; Marcel Dekker, New York, 2001).

37. V. F. Vasilevskii and V. I. Mazhukin, "Numerical Calculation of Temperature Waves with Weak Discontinuities Using Dynamically Adapted Grids," Differ. Uravn. **25**, 1188–1193 (1989).

38. D. A. Anderson, J. C. Tannehill, and R. H. Pletcher, *Computational Fluid Mechanics and Heat Transfer* (Hemisphere, New York, 1984).

39. J. B. Bell and G. R. Shubin, "An Adaptive Grid Finite Difference Method for Conservation Law," J. Comput. Phys. **52**, 569–591 (1983).

40. E. R. Benton and G. W. Platzman, "A Table of the One-Dimensional Burgers Equation," Quarterly Appl. Math. **30**, 195–212 (1972).